1. RE Output Fluctuation

RE Output Identification and Prediction

One reason why renewable energy (RE) cannot be handled easily is that RE output varies unintentionally due to natural condition. RE output prediction is, of course, to predict RE output in near future using climate prediction and so on, and has been recently considered as indispensable for reliable electric power system operation. Since any prediction cannot get rid of some error, knowing error level of each prediction method is important.

The meaning of the words “RE output identification” is not easily imaginable but is roughly considered as follows. It will be not so easy to measure and make sum of existing all REs. Although the way “measuring” is the most orthodox method, number of highly penetrated RE will be tremendous and REs are geographically diverse in very wide area. “Measuring” all REs is not realistic. Therefore, engineers wonder whether “identifying” output of all REs using output of fewer sample REs is possible. The way “identification” is not so orthodox as “measurement”. But certainly total RE output can be approximately presumed. Of course identification cannot get rid of some error, but the identification error is hoped to be smaller than prediction error because identification does not handle future phenomena. Thus, output identification has become regards as indispensable not only for reliable power system operation but also for assessing accuracy of each output prediction method.

RE output identification method is quite simple as shown in Fig. 1.1. Magnification factor is easily calculated from total capacity of sample REs and all REs. On the contrary, smoothing factor was not clearly understood even in 2010 in spite of 10 years research.

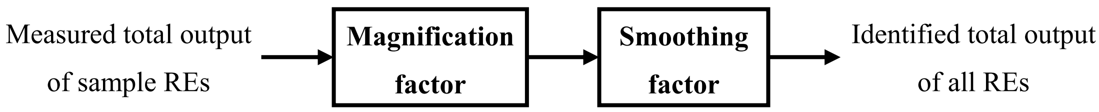

Fig. 1.1 Method of RE Output Identification

Traditional Way: Inductive Method

For understanding smoothing effect, it is indispensable to measure time variation of output. One example of solar irradiance with the largest fluctuation during March to May 2010 is shown in Fig. 1.2.

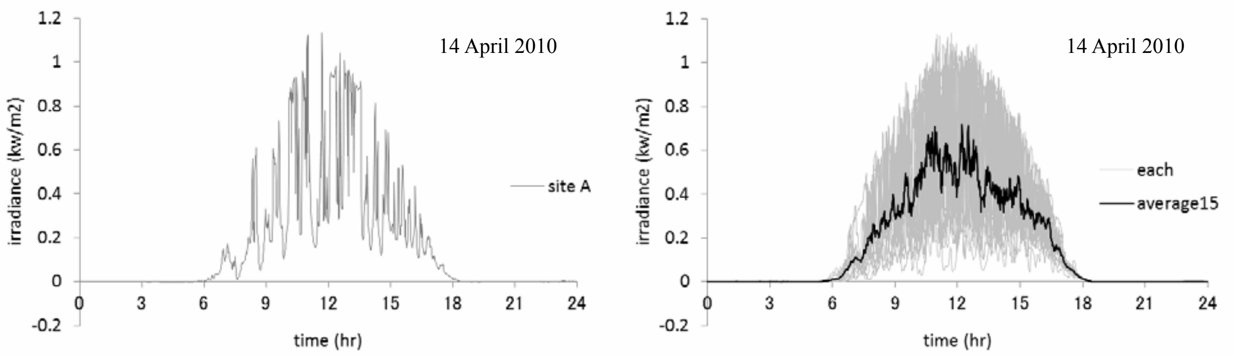

Fig. 1.2 Measured Irradiances of Hokuriku 15 Sites

Fluctuation width of site A is very large and is almost equal to maximum irradiance. Overlaying 15 sites’ data, plotting area becomes gray and individual curve cannot be recognized. Fluctuation of individual site is quite large. However, average irradiance of the 15 sites is quite smoothed out. Thus, smoothing effect can be visually recognized, but quantitatively analysis is not possible yet.

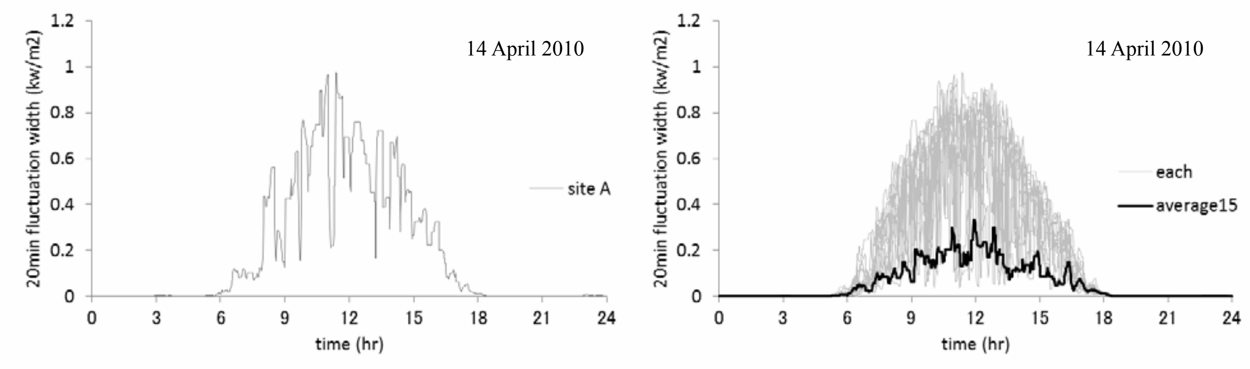

Fig. 1.3 20min Fluctuation Width of Hokuriku 15 sites

For quantitatively analysis as the first step in Japan, 20min fluctuation width that is the difference of the maximum and the minimum of continuous 20min time sequential output data was calculated. That of 14 April 2010 is shown in Fig. 1.3. Although smoothing effect is visually understood, quantitatively analysis is not possible yet.

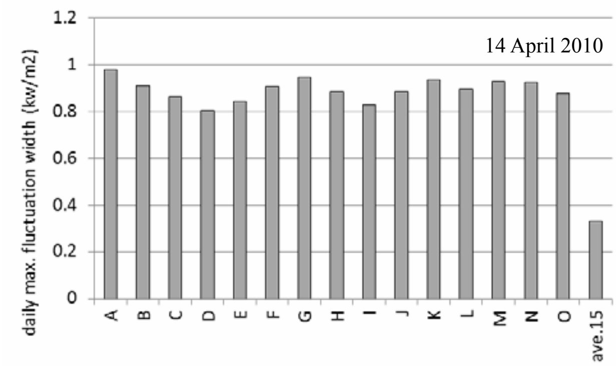

Fig. 1.4 Daily maximum 20min fluctuation width

Therefore as the next step, daily maximum value of the 20min fluctuation width was calculated. That of 14 April 2010 is shown in Fig. 1.4. Thus, smoothing effect can be quantitatively evaluated whatever may be the way. Values are as follows.

15 sites average of fluctuation width: $\Sigma(\varDelta P)_{1\sim15} / 15 = 0.894342$

Fluctuation width of 15 sites average output: $\varDelta(\Sigma P_{1\sim15}) / 15 = 0.332373$

Perhaps smoothing effect is best defined as follows. Here, $\varDelta(\Sigma P)$ means fluctuation of total output, and $\Sigma(\varDelta P)$ means sum of individual fluctuation.

$$\text{Smoothing Effect} = \frac{\varDelta(\Sigma P)}{\Sigma(\varDelta P)}$$

In case of the example, smoothing effect is calculated as follows.

$$\text{Smoothing Effect} = \frac{\varDelta(\Sigma P)}{\Sigma(\varDelta P)} = \frac{\varDelta(\Sigma P_{1\sim15}) / 15}{\Sigma(\varDelta P)_{1\sim15}) / 15} = \frac{0.332373}{0.894342} = 0.371639$$

It is already known that smoothing factor becomes as follows if fluctuation of each site is perfectly independent.

$$\text{Smoothing effect} = 1 / \sqrt{15} = 0.258199$$

Index here used "daily maximum 20min fluctuation width" intends to assess short term fluctuation, but does not necessarily represent perfectly random (independent) fluctuation, because a part of much slower and larger variation is also included in the index.

As the result, smoothing factor calculated in the case (around 0.37) is applicable the case only. In another case, smoothing factor must be measured and calculated again from the beginning. As an examination, smoothing factor of 7 sites (that are covering Hokuriku area as well as the 15sites) out of the 15sites is calculated as follows.

$$\text{Smoothing effect} = \frac{\Delta(\Sigma P)}{\Sigma(\Delta P)} = \frac{\Delta(\Sigma P_{1\sim7}) / 7}{\Sigma(\Delta P)_{1\sim7}) / 7} = \frac{0.550291}{0.893004} = 0.616225$$

The result (around 0.62) is quite different from that of 15 sites. Irradiance and 20min fluctuation width of each site and average are shown in Fig. 1.5 and 1.6 respectively. Their appearance is certainly different from that of 15 sites case.

The reason why much labor can produce very little fruits is the fact that employed analysis method is a kind of "inductive method", which cannot create general theory that is applicable almost any case. Inductive method can create empirical theory after very many case studies, for which expensive wide area measuring must be continued for a very long time. Thus, inductive method does not work well for rapid and economical learning of smoothing effect.

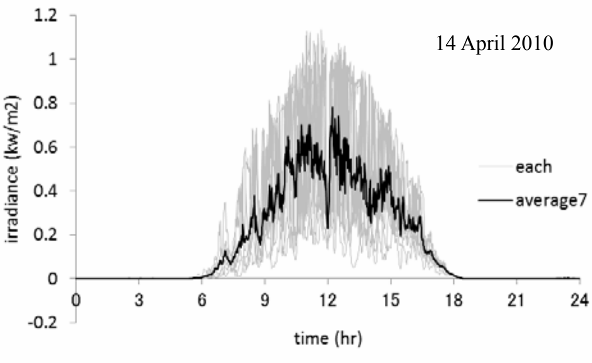

Fig. 1.5　Irradiance of Hokuriku 7 sites

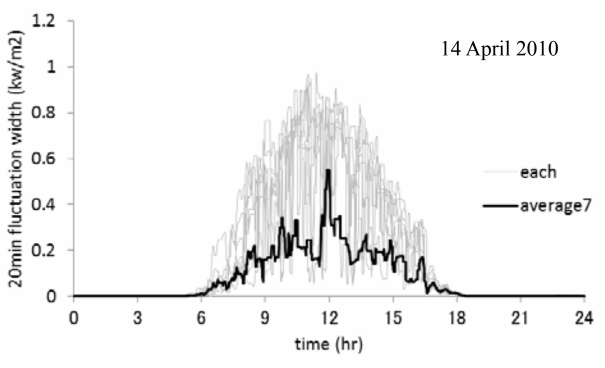

Fig. 1.6　20min fluctuation width of Hokuriku 7 sites

Transfer Hypothesis: Deductive Method [(1), (2), (3)]

As the contrary approach of "inductive method", "deductive method" exists. Deductive method proposes a hypothesis such as "RE smoothing effect can be expressed as follows…" If results logically conducted from the hypothesis agree with measured facts, the hypothesis become reliable by one step. Proposing and verifying hypotheses are fundamental approach of science. For proposing a hypothesis, insight into natural phenomenon is essential. If the insight is wrong, the hypothesis is also wrong, and as the result, the hypothesis will be denied by measured facts.

Transfer hypothesis proposed by the author is expressed as follows.

$$\text{Smoothing factor} = \frac{\Delta(\Sigma P)}{\Sigma(\Delta P)} = \left| \frac{1 + j\,Tx\,f/\sqrt{N}}{1 + j\,Tx\,f} \right| \tag{1.1}$$

Here, j is imaginary unit, f is fluctuation speed, and N is number of RE. Tx is a constant unique number for the studied area and named as "Transfer Period". Transfer hypothesis assumes that slower fluctuation than Tx is coherent, but faster fluctuation begins to lose coherence and transfers toward random fluctuation. Slope of transfer is assumed as proportional to -1 time powered fluctuation speed as very often seen in natural phenomena. Tx becomes larger when studied area is larger.

The author has written the conclusion at the beginning. Of course, there is a long way to be walked to reach the conclusion. As the beginning, it must be noticed that characters of slow coherent fluctuation and fast random fluctuation are already known as Table 1.1.

Table 1.1 Character of Slow and Fast Fluctuation

	Slow fluctuation	Fast fluctuation
Fluctuation of 2 REs	Coherent	Random
Fluctuation of Multiple REs	Sum of each RE fluctuation	Pythagoras sum of each RE fluctuation
Fluctuation of highly penetrated RE	Proportional to RE capacity	Proportional to square root of RE capacity

Unknown matter may be explained by multiple matters already known. RE fluctuation will be explained by combination of slow and fast fluctuations. The question is what rules the combination.

Elements affecting smoothing effect are listed up as follows sorted by importance.

1. Fluctuation speed — Fast fluctuation shows strong smoothing effect
2. Size of area — Large area shows strong smoothing effect
3. Number of REs — Large number of REs show strong smoothing effect
4. RE distribution — Even distribution case shows strong smoothing effect
5. The others — Statistical noise for the time being

Character of RE fluctuation is quite different by speed. Real fluctuation includes various speed elements simultaneously. As the result, speed must be main variable and make horizontal axis of graph expression. Since size and number are kept constant in a case study, they are considered as parameters. As introduced later, uneven distribution makes smoothing effect weaker but slightly. However, there are many people who regard distribution as most important although fluctuation speed is not sufficiently considered.

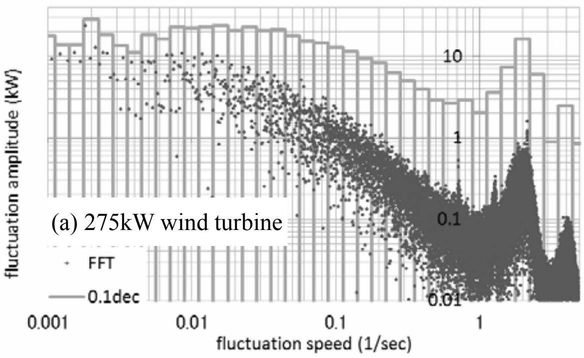

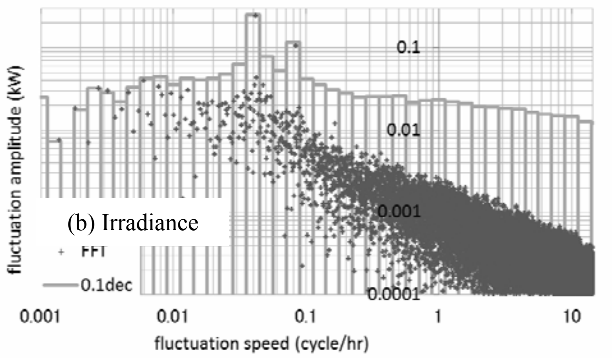

Fig. 1.7 Output fluctuation spectra of renewable energies

It is spectrum that has fluctuation speed as main variable on horizontal axis. FFT (Fast Fourier Transform) is employed for transforming time sequential data to spectrum. But result of FFT is discrete spectrum. As examples, FFT result of (a) a 275kW wind power fluctuation and (b) irradiance fluctuation at a site are shown in Fig. 1.7 (usually logarithm axis is employed in both vertical and horizontal). Number of data having poor meaning at fast fluctuation is tremendous, and each dot is hardly recognized. Therefore, some smoothing method is needed. And the method is hoped to have physical meaning.

Here, as a smoothing method having physical meaning, 1/10 decade method is introduced. 10 times section on logarithm speed axis is divided into 10 equal bands. Pythagoras sum of fluctuation elements included each band is employed as height of the band. All bands contact side by side as shown in Fig. 1.7. The method sometimes called as 1/3 octave method. Using the method, 1/f fluctuation that is often seen in natural phenomena is expressed flat. In the figure (a), 0.1/sec fluctuation or slower is almost flat by 1/10 decade expression. Faster fluctuation decreases proportional to -1 time powered fluctuation speed. The decrease is also often shown in natural phenomena. In the case, main cause is inertia of propeller. At more faster fluctuation peaks are observed. They are derived from so called “tower shadow effect”. In the figure (b), fluctuation is almost flat except two peaks, which is derived from 24 hr cycle irradiance change by rotation of the globe. 1/10 decade method is praised and widely used in acoustic field due to these excellent characters. Frequency band standard is set in IEC. Spectrum analyzer is typical equipment using 1/10 decade method. However, these facts are not written texts of spectral analysis. Since expression of 1/10 decade method seen in the Figure is very laborious, folded line linking center of column upper end is employed hereafter.

Spectra of Hokuriku 15 sites by continuous time sequential measured data in spring three months are shown in Fig. 1.8. 15 Spectra curve are almost equal. That is, so long as calculating long term average, increasing number of measuring sites is not cost effective.

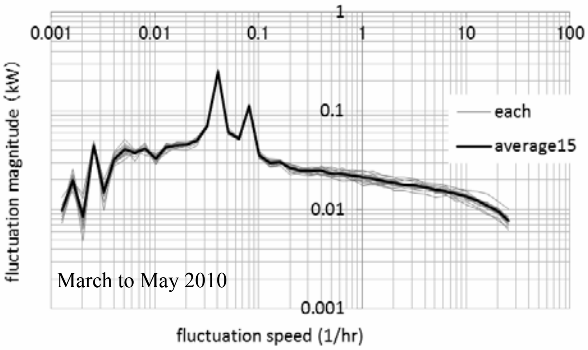

Fig. 1.8 Irradiance spectra of Hokuriku 15 sites

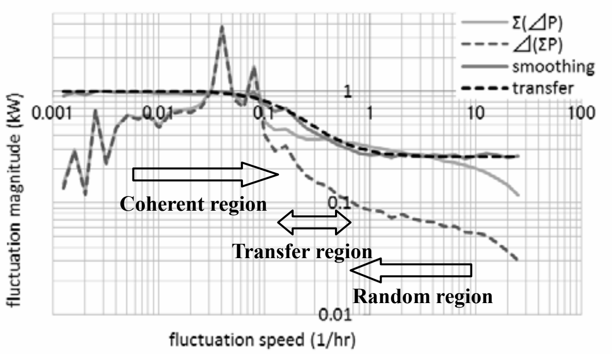

Fig. 1.9 Transfer hypothesis represents smoothing factor

In equation (1.1) that defines transfer hypothesis and smoothing factor, as fluctuation magnitude that is signed by $\varDelta$ in the equation, 1/10 decade spectra can be also adopted instead of daily maximum 20min fluctuation width. The equation is expressed as a function of fluctuation speed in case of 1/10 decade spectra, while the equation results a real number in case of 20min fluctuation width. Smoothing factor by Hokuriku 15 sites spectra are calculated as Fig. 1.9. Transfer hypothesis employing 7.2 hr as T_x can represent smoothing factor very well. Two sharp peak seen in $\Sigma(\varDelta P)$ and $\varDelta(\Sigma P)$ spectra are not seen in smoothing effect and transfer hypothesis. Since equation (1.1) has effect of daily irradiance cycle both in numerator and dominator, irradiance cycle effect is canceled. The reason why 3 months of long continuous time sequential data are used is to confirm that very slow fluctuation is certainly coherent.

Transfer hypothesis contains only one parameter Tx to be identified from measured data. Tx is a constant unique for the studied area, and do not vary much in another season or if RE number increase. The character tells that Tx hits the true nature of smoothing effect. On the contrary, smoothing factor calculated by inductive method varies largely case by case. The reason why Tx is kept constant even if RE number increases is explained as follows. Two REs, P and Q cover area A as shown in Fig. 1.10. A new RE, R joins in area A. Distance between R and the nearest existing site from R (It is P in this case.) must be shorter than distance between P and Q (D), if P and Q cover area A. Fluctuations of P and Q are coherent at slower speed than Tx. Since R is nearer to P than Q, fluctuations of R and P must be coherent in slower speed than Tx. Thus, fluctuation of newly joined RE in area A is necessarily coherent with fluctuation of P and Q in slower speed than Tx. (Q. E. D.)

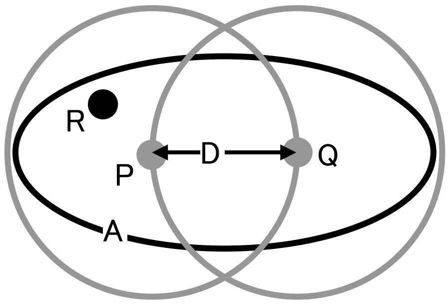

Fig. 1.10　The reason why Tx does not vary

Expression of equation (1.1) means a kind of low pass filter, but it is unique that the equation is expresses as absolute value and has no phase shift. Ordinary low pass filter has some phase delay due to inertia, coil, and so on, and usually expresses equation (1.1) before taking absolute. Since smoothing effect is realized instantly by RE geographically diverse, any phase delay and time delay appear. If absolute of the equation is ignored, a large distortion will appear in daily output presumption curve when RE highly penetrates.

When Number of Sites Increases N to M

Using equation (1.1) that defines transfer hypothesis, fluctuation of N sites' total output $\Delta(\Sigma P_{1\sim N})$ can be expressed as follows.

$$\Delta(\Sigma P_{1\sim N}) = N\,(\Delta P)_{ave} \left| \frac{1 + j\,T_x\,f/\sqrt{N}}{1 + j\,T_x\,f} \right| \qquad (1.2)$$

Here, $(\Delta P)_{ave}$ is one site's average spectrum. Since long term spectra of all 15 sites are nearly equal as shown in Fig. 1.8, it is reasonable that sum of all 15 sites' spectra $\Sigma(\Delta P)_{1\sim N}$ is approximately expresses as $N\,(\Delta P)_{ave}$. When number of sites increased to M, sum of all M sites' spectra $\Delta(\Sigma P_{1\sim M})$ can be written as

$$\Delta(\Sigma P_{1\sim M}) = M\,(\Delta P)_{ave} \left| \frac{1 + j\,T_x\,f/\sqrt{M}}{1 + j\,T_x\,f} \right| \qquad (1.3)$$

Dividing equation (1.3) by equation (1.2), amplification factor when number of RE sites increases N to M as follows. The amplification factor consists of magnification factor and smoothing factor in Fig. 1.1.

$$\frac{\Delta(\Sigma P_{1\sim M})}{\Delta(\Sigma P_{1\sim N})} = \frac{M}{N}\left|\frac{1 + j\,T_x\,f/\sqrt{M}}{1 + j\,T_x\,f/\sqrt{N}}\right| \qquad (1.4)$$

Assume that we have only three measured data at site A in Toyama, site B in Kanazawa, and site C in Fukui. Tx was calculated as 7.8 hr from those three data even though accuracy is somewhat lower than 15 sites case. Multiplying spectrum of the three sites' total output $\Delta(\Sigma P_{1\sim 3})$ by the amplification factor defined by equation (1.4) employing the calculated 7.8 hr Tx , spectrum of the all 15 sites' total output $\Delta(\Sigma P_{1\sim 15})_{ide}$ can be identified. By the way, we have true spectrum $\Delta(\Sigma P_{1\sim 15})_{true}$, therefore we can assess the accuracy of 3 sites to 15 sites identification. The result is shown in Fig. 1.12. Although number of sites whose data were used for identification is small as 3, accuracy is not so bad. The reason of not bad accuracy is the fact that long term spectra of all sites are very similar as shown in Fig. 1.8.

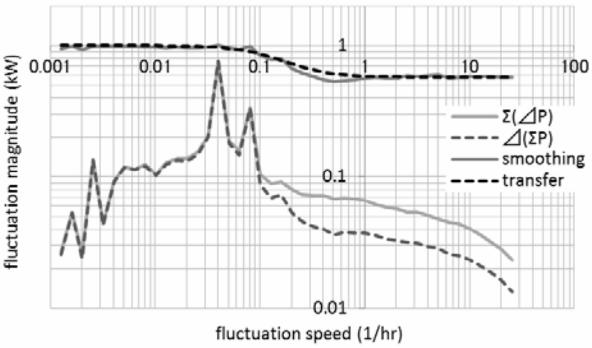

Fig. 1.11 Smoothing effect and transfer hypothesis of the 3 sites

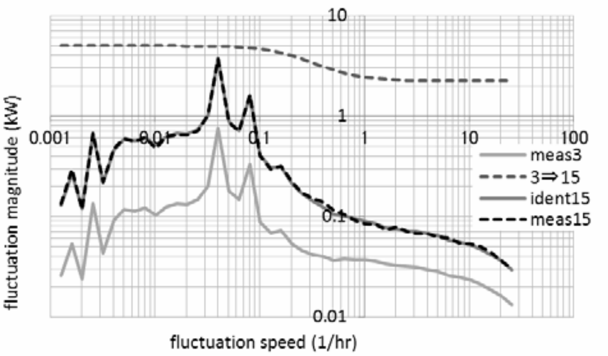

Fig. 1.12 identified and measured spectra of 15 sites' total

Thus, hypothesis can be verified, if something that is possible to be checked by measured data or observed facts can be logically deduced from the hypothesis. Sometimes hypothesis may be falsified. It is quite important for scientific way that hypothesis is verified even only one truth. Hypothesis that is not verified yet is a mere random remark.

Application to Time Sequential Data

Amplification factor when number of RE sites increase N to M can be expresses as gain and low pass filter as equation (1.1). The fact means that the amplification factor can be applied not only to spectrum but also to time sequential data. But it must be noticed that the amplification factor has no phase shift. Therefore, some techniques are needed as shown in Fig. 1.13.

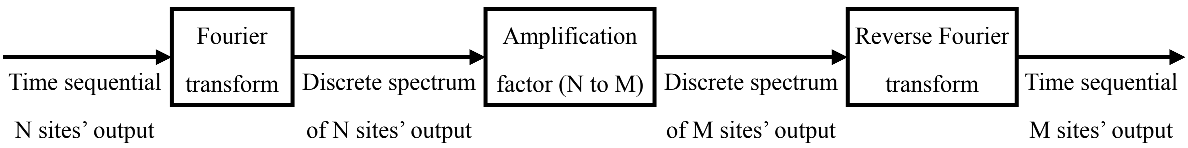

Fig. 1.13 Application of transfer hypothesis to time sequential data

Time sequential N sites' total output $\Sigma_N P(t)$ is once transformed toward discrete spectrum with gain and phase data through FFT. The result spectrum is multiplied by the amplification factor toward identified M sites' spectrum. The result is transformed toward time sequential data of M sites' identified total output through reverse FFT. It must be noticed that phase data of spectrum through FFT have meaning and the phase data must not be ignored as zero, and any smoothing method for discrete spectrum (such as 1/10 decade method) are forbidden.

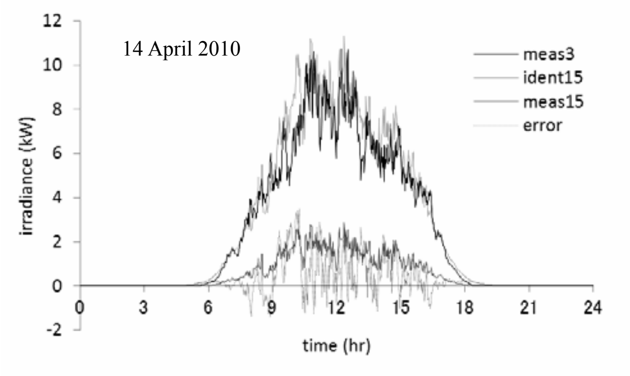

Fig. 1.14 Identified and measured time sequential output

Usually time sequential data are analyzed in 1 day length. Therefore as the matter of course, suitable Tx must be different from Tx used in spectral analysis in long term. In addition geographical difference will be larger at shorter time sequential data. Therefore, identification accuracy employing 1day length data must be worse than that employing long term data. On trial, 1 day total irradiance of Hokuriku 15 sites is identified from 1 day irradiance 3 out of the 15 sites. The result is shown in Fig. 1.14. Average irradiance during 6 to 18 hr is 4.82kW in 15 sites measured data. Identification RMS error is 1.03kW, which is up to 21.3% of average irradiance. However so long as seeing the Figure, error seems not fatally large. The large RMS error is brought by the fact that only 3 sites data was used for identification. Similarly identifying 5 times larger number of sites, identification of 75 sites using 15 sites data will bring much smaller RMS error, but the estimation is not able to be verified now because of shortage in measuring sites number. Verification of transfer hypothesis in case of time sequential data must stop here today.

When RE Highly Penetrates

By analyses above output identification when RE highly penetrates becomes possible. Assuming 53GW capacity of photovoltaic (PV) penetrates in Japan in 2030, 154MW capacity of PVs will join in Hokuriku area. Assuming all PVs are home use and having 4kW capacity, number of PVs are calculated as follows.

1540000kW / 4kW = 385000 sites

Therefore, total output of M = 385000 sites is to be identified using N = 15 sites measured data. Tx is assumed as 7.2 hr, which was derived another analysis of 15 sited data and slightly shorter than the result above. Because the author thought that shorter Tx will bring more pessimistic result.

We hope to compare fluctuation of highly penetrated RE to demand fluctuation. In case of spectral analysis it must be noticed that spectrum of continuous long term contains data at night when PV output is zero. In a fine day PV will draw daily output curve as shown in Fig. 1.15, which is almost upper half of sine wave. Daily average irradiance is $1/\pi$ of peak at noon. If the sun always stands at right south direction, daily average irradiance will be π times larger than the fine day, and as the result fluctuation also will be π times larger. Therefore, when comparing to demand fluctuation, PV output fluctuation must be assessed π times larger.

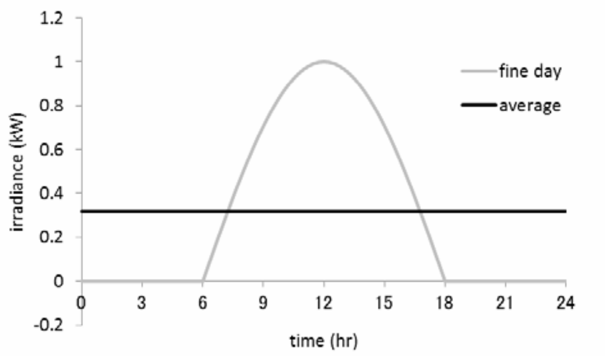

Fig. 1.15 Daily irradiance curve in a fine day

Considering the notice above, all PV fluctuation spectra are assessed by π times larger here. Fluctuation spectrum of highly penetrated PVs presumed from 15 sates measured data was calculated as shown in 1.16. M/N ratio is so large that 15 sites data are drawn in kW unit and data highly penetrated are drawn in MW unit. 1 hr cycle or faster highly penetrated PV fluctuation that obstructs system frequency regulation is slightly smaller than demand fluctuation. System frequency regulation issue that had been so loudly spoken is found, in fact, as not so serious problem. That has not become clear till transfer hypothesis are employed.

Daily output curve of highly penetrated PVs were presumed from 15 sites total irradiance curve of one day that shows the largest fluctuation. The result is shown in Fig. 1.17 comparing output curve without considering smoothing effect. Since total output of highly penetrated PVs are quite smoothed out even on the day showing the largest irradiance fluctuation, severe power system operational obstacle is hardly imagined. On the contrary, the increasing PV output at morning will be helpful to cancel the increasing demand.

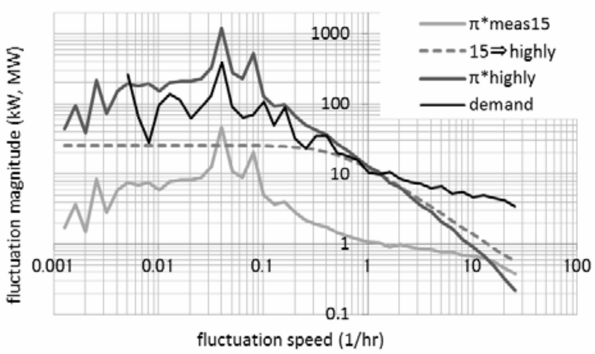

Fig. 1.16 Presumed spectrum of highly penetrated PVs

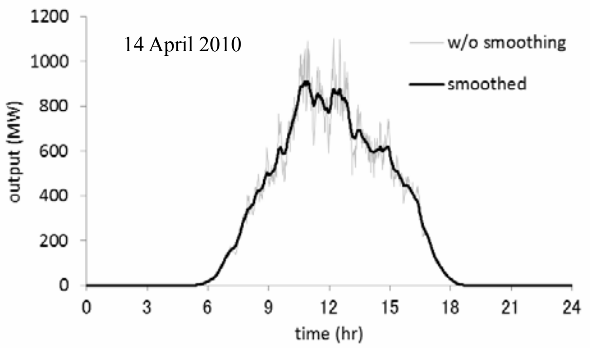

Fig. 1.17 presumed daily output of highly penetrated PVs

In fluctuation spectrum of highly penetrated PVs, fast fluctuation from minutes to 1 hr that obstructs system frequency regulation exists in transfer region where magnitude is proportional to -1 time powered speed. In transfer region fluctuation is not coherent but is not random. In smoothing effect of 15 sites (already shown in Fig. 1.9) 1 hr period or faster fluctuation exists in random region. As number of RE increases, transfer region expands to right side, and as the result random region shrinks. From the fact that 1 hr period or faster fluctuation concerning system frequency regulation exists in random region in case of fewer sample RE measured data, one may carelessly believe that 1 hr period or faster fluctuation always exists in random region and as the result may underestimates fast fluctuation in case of highly penetrated RE. By these reason, inductive methods becomes more dangerous when RE penetrates higher.

Identify T_X without Measurement

It is transfer swing period T_X that performs an important role in transfer hypothesis. A close relationship between T_X and size of the region studied must exist. If T_X can be presumed from the size, measurement for identifying T_X becomes useless. It is quite convenient. For the purpose, ${}_{15}C_2$ = 105 pairs of 2 sites' distance D and transfer swing period T_X of the 2 sites were prepared, as shown in Fig. 1.18. A theoretical formula as follows is introduced. It contains two unknown parameters: T_{X2M} and D_0.

$$T_{X2} = T_{XM}\ \{1 - \exp(-D / D_0)\}\quad \text{(hr)} \qquad (1.5)$$

The equation is approximated as follows.

$$T_{X2} = T_{X2M} \qquad \text{at large D (satulate)}$$

$$T_{X2} = T_{X2M}\ (D/D_0) \qquad \text{at small D (slope)}$$

T_{X2M} can be identified by average of D>130km data as 10.08km.

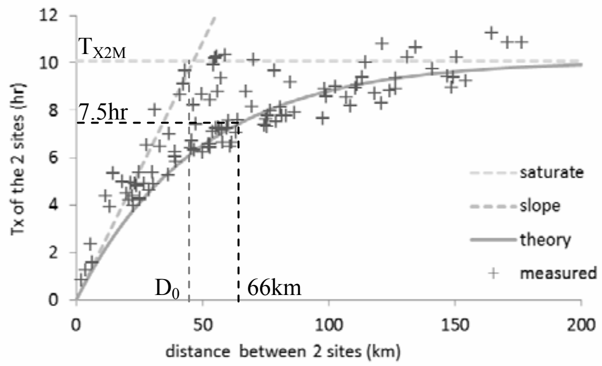

Fig. 1.18 Transfer period and distance of 2 sites (wide)

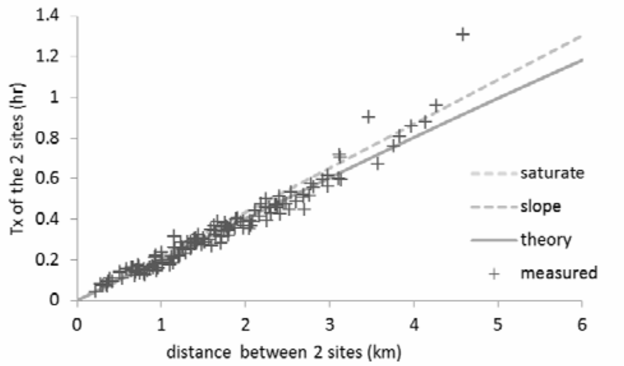

Fig. 1.19 Transfer period and distance of 2 sites (narrow)

For identifying D_0, many measured data at small D are necessary. Then, ${}_{17}C_2$ = 136 pairs of data were prepared by measuring in a small area fed by a feeder. The results are shown in Fig. 1.19. For the 136 pairs, D_0 was identified as 48.05km so that sum of square error between measured value and theoretical formula value becomes to the minimum.

Here, the reason why T_{X2} is proportional to D is thought. When inhabitable area of the region studied S km^2 and mesh interval on which PVs locate is D km, number of PVs is $N = S/D^2$. Swing period at which fluctuation of all reaches to random is expresses as follows by using a transfer swing period T_{XX}.

$$T_Y = T_{XX} / \sqrt{N} = T_{XX} / \sqrt{(S/D^2)} = T_{XX}\ D / \sqrt{S}$$

Since in case of 2 sites, T_{X2} is $\sqrt{2}$ times of T_Y above as follows.

$$T_{X2} = T_{XX}\ D / \sqrt{(S/2)}$$

Thus, it is demonstrated that T_{X2} is proportional to D. The introduced T_{XX} in Hokuriku region can be calculated as follows.

$$T_{XX} = (T_{X2M}/D_0)\ \sqrt{(S/2)} = (10.08/48.05)\ \sqrt{(4300/2)} = 9.7\ \text{hr}$$

T_{XX} is close to T_{X2M}, but it is no more than a coincidence.

Characteristic size of Hokuriku region is, since distance between Tomari at the east end and Tsuruga at the west end is 198 km, 198/3 = 66 km, by the principle of Fig. 1 (1/3 of the major axis). T_X corresponding D = 66km is 7.5 hr. Theory is found to be well harmonized.

Furthermore in Hokuriku region, seasonal variation of T_X[8] and T_X in those days with large fluctuation[9] were calculated by the author, but never deviated from 7.5 hr much.

The author has a motive to verify such a not meaningful theory. Transfer theory assumes that transfer slope of magnitude from coherent to random is proportional to -1 time powered speed. From the assumption the result that transfer period is proportional to distance for 2 sites if distance is small is conducted. If the result agree with measured data well, the assumption is verified. By analysis above, the assumption that transfer slope is proportional to -1 time powered speed is verified.

Uneven Distribution of RE [4]

There are many Engineers who seriously believe that distribution of RE affects smoothing effect very much. The belief is considerable if RE output is quite different by location. However, at least on long term continuous spectrum, RE output differs little by location as shown in Fig. 1.18. Therefore, remainder influence of uneven distribution are only discount of smoothing effect due to uneven distribution and slightly increase of fast fluctuation in total output. Perhaps it is quite possible that uneven distribution does not affect RE total output so much as area size and number of RE.

Slightly extending transfer hypothesis, uneven distribution can be considered like Fig. 1.20, in which one block consists of core with many REs and space.

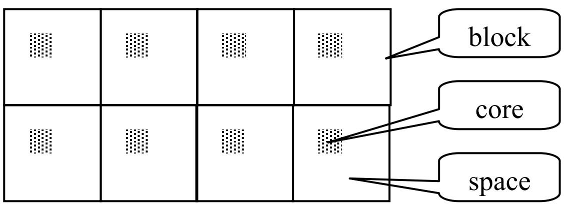

Fig. 1.20 Core and space structure

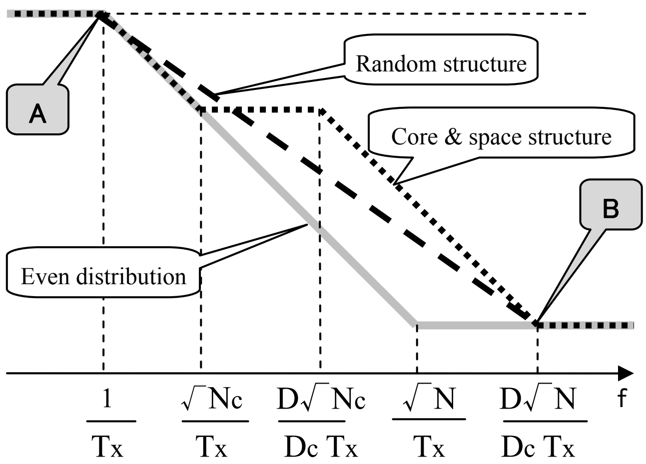

Fig. 1.21 Smoothing effect in uneven distribution

Smoothing effect in core and space structure can be expressed like Fig. 1.21. Here, N is number of REs, D is distance of neighboring REs in even distribution case, Nc is number of cores, and Dc is distance of neighboring REs in cores. As matter of course, Nc is further smaller than N, and Dc is further smaller than D. Fast fluctuation magnitude become larger than even distribution case.

According to Fig. 1.21, smoothing effect in core and space structure is expressed as follows. In the right side, left half means inter-block smoothing effect and right half means intra-block smoothing effect.

$$\text{Smoothing effect} = \left| \frac{1 + j\dfrac{Tx\,f}{\sqrt{Nc}}}{1 + j\,Tx\,f} \; \frac{1 + j\dfrac{Dc\,Tx\,f}{D\sqrt{N}}}{1 + j\dfrac{Dc\,Tx\,f}{D\sqrt{Nc}}} \right|$$

Suppose total 1540MW capacity of RE penetrates in Hokuriku with 4300km^2 inhabitable area, and capacity of single RE is 4 kW. Number of REs: N is calculated as follows.

$$N = 1540000\text{kW} / 4\text{kW} = 385000$$

Suppose that size of single block is 10km^2. Then Number of cores is calculated as follows.

$$Nc = 4300\text{km}^2 / 10\text{km}^2 = 430$$

Distance of neighboring REs in even distribution case is calculated as follows.

$$D = \sqrt{(4300\text{km}^2 / 385000)} = 0.105683 \text{ km}$$

Distance of neighboring REs in cores is supposed as follows.

$$Dc = 0.02 \text{ km}$$

Thus, all parameters are prepared. Using these parameters, spectra are calculated as Fig. 1.22. To compare with demand fluctuation, all RE spectra are π times multiplied. Several minutes' period or faster fluctuation becomes around 3 times larger than even distribution case. However, 1 hr period or faster RE fluctuation does not exceed demand fluctuation.

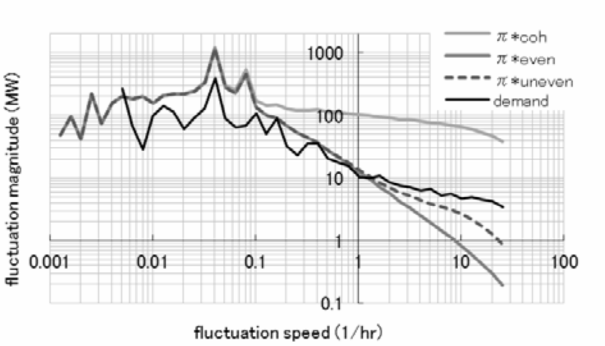

Fig. 1.22 Fluctuation spectra of core & space structure

$$\text{Smoothing factor} = \left| \frac{1 + j\left(\dfrac{Dc\,Tx\,f}{D\sqrt{N}}\right)^K}{1 + j\,(Tx\,f)^K} \right| \qquad (1.6)$$

However, existing houses do not distribute in order as Fig. 1.20 but distribute randomly. Only Points A and B in Fig. 1.21 can be confirmed by measurement or observation. If so, it must be realistic and practical to roughly draw a line from A to B as spectrum of uneven distribution. As the result, smoothing factor in random uneven distribution case is expressed as equation (1.6).

One unknown parameter: K exists in equation (1.6) to be identified. Noticing that smoothing factor at very fast fluctuation is equal in even distribution case and uneven distribution case, parameter K must fulfill the condition as follows.

$$\left(\frac{Dc}{D\sqrt{N}}\right)^K = \frac{1}{\sqrt{N}}$$

Thus, parameter K is calculated as follows.

$$K = \frac{\log \frac{1}{\sqrt{N}}}{\log \frac{Dc}{D\sqrt{N}}} \qquad (1.7)$$

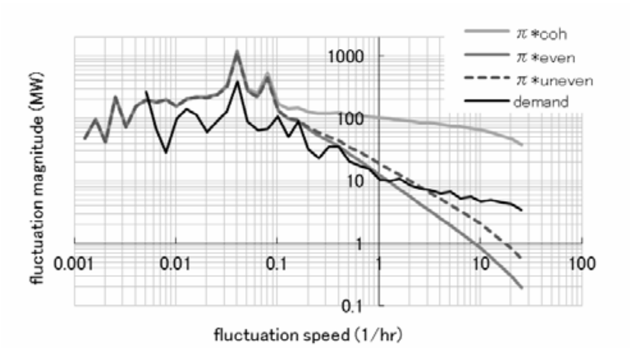

Fig. 1.23 Fluctuation spectra of random structure

1/10 decade spectra when 1540MW capacity of REs penetrates in Hokuriku by random uneven distribution are shown in Fig. 1.23. Likely above RE fluctuation spectra are π times multiplied for comparison with demand fluctuation. Magnitude at several hr period or faster fluctuation of RE is around 2 times larger than even distribution case. Around 30 min period or slower RE fluctuation becomes larger than demand fluctuation. However, it must be noticed that distance of neighboring REs in densely distributed region is chosen very short as 20m for conservative assessment. Fast fluctuation must be slightly smaller.

Problems of Traditional Way (7)

If inductive traditional way has no problem, the author will follow the way to avoid laborious task such as cutting out another deductive way. Typical difference of the two ways is drawn in Fig. 1.24. Traditional way has obvious problems. The first is extracting an index “daily maximum 20min fluctuation width” from fewer sites’ measured data, and presuming the index of highly penetrated RE by processing the fewer sites’ index. Whatever splendid index it may be, any index is no more than a real number whose information amount is quite smaller than original time sequential data. Therefore, traditional way intends to presume the answer using very poor amount of information, and as the result, presuming accuracy by traditional way must be poor.

On the contrary, transfer hypothesis does not lose information amount of fewer measured data for presuming the time sequential output of highly penetrated RE. The way is promising in accuracy.

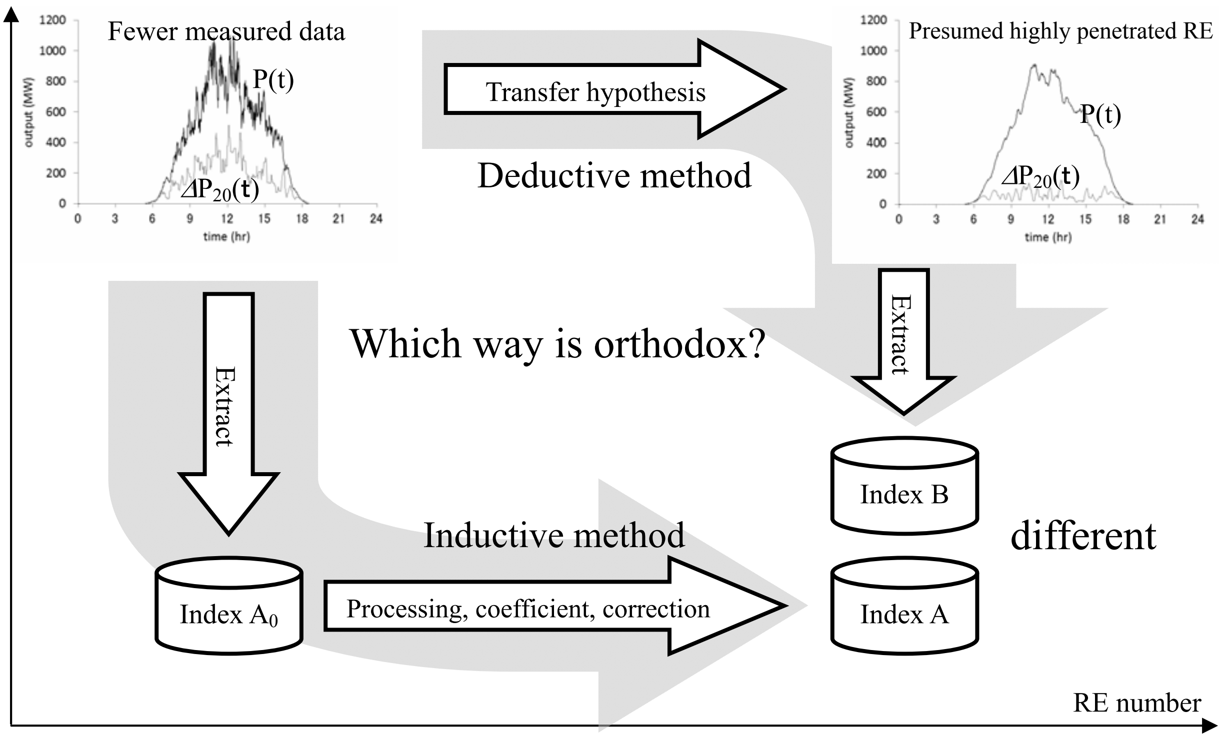

Fig. 1.24 Difference of traditional way and transfer hypothesis

As an example, asynchronism reveals low presuming accuracy of traditional way, which perhaps assume that “daily maximum 20min fluctuation width” of highly penetrated RE will appear in the same time when that of fewer measured REs appears.

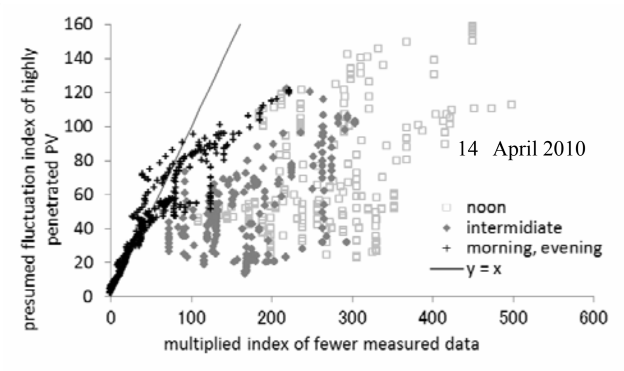

Fig. 1.25 Indices of 15 sites and high penetration

As a trial, the index of 15 measured sites and index of presumed highly penetrated RE are compared as shown in Fig. 1.25. Times when the index shows the highest value are apparently different between 15 sites and highly penetrated. If smoothing effect does not work at all, data will be plotted on y = x line in the figure. Data in the morning and at evening almost stand on the y = x line. On the contrary, smoothing effect strongly works at noon. In Fig. 1.24, it is observed that variation range of the index becomes narrower as RE highly penetrates.

Translation from Irradiance to Output

Methods introduced above are measurement and prediction of irradiance. For practical use, irradiance must be translated to output. Employed researchers propose sampling measurement of existing PVs. However, the method has difficulties in time and cost. On the contrary, the author, an artisan of power system, proposes to use past monthly buying records of PVs that utilities necessarily have with past measured irradiance for conducting the translation coefficients. Since the method uses only past recorded data, difficulties in time and cost will be quite small. Some utilities approve the author's method, but sampling measurement has not started yet.

Battery LFC [5], [6]

For regulating system frequency, outputs of generators for "regulation" use are automatically adjusted by "LFC" (Load Frequency Control). Demand fluctuation with several minutes period is compensated by LFC. Outputs of the other generators are also at least manually adjusted so that outputs of regulation use generators do not reach upper or lower limit and always stay within arrowed output band. As the result, total output of all generators always follows load variation. This is "load following". Slower and larger load variation can be forecasted in advance. For forecasting error and accidental generator trip some "reserve" is prepared for reliable system operation. "Negative reserve" is also necessary in case of unexpected low demand, unexpected large RE output, and so on.

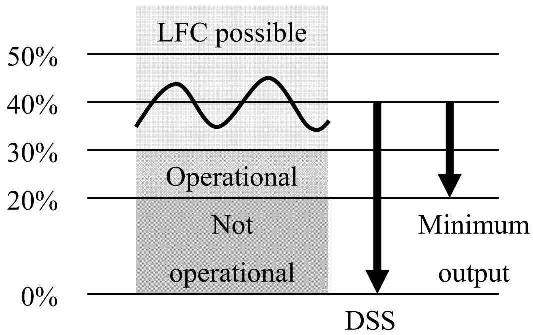

Fig. 1.26 Operational output of thermal generator

In future with high RE penetration, some amount of battery is possible to be employed. In such a case, using battery as regulation source is more cost efficient than using mare storage. Typical possible output band of thermal generator is shown in Fig. 1.26. For ±5% regulation use, average output must be around 40% or more. If regulation is not needed, output can be reduced to 20%, or the generator can be stopped. As the results, reduced output 20 to 40% can be used as "negative reserve".

The author regards output curtailment on nuclear power as ultimate "negative reserve". Although ramp rate of output variation is limited due to safety of fuel rod, output change is technically possible even in nuclear power. Output change is already done in foreign countries and once done even in Japan successfully. Although fuel cost of nuclear power is very low, keeping maximum output of nuclear power will lose reason when RE highly penetrates, because fuel cost of hydro, wind, and solar power is zero.

Curtailment of REs is another method for preparing "negative reserve". Remember that energy that is gift from nature was thrown away when not needed in ancient wind mill and water mill. However, output control of tremendous many REs seems not practical.

If problems around "reserve" are solved, problems around "load following" and "regulation" remain. Since those problems are derived from fast fluctuation of demand and RE, using battery for solution is a realistic method. Batteries are excellent power (kW) source but quite expensive energy (kWh) source, therefore, are suitable for short term phenomena.

Even power source use of battery seems economically hard for local small utilities. However, in large utilities or interconnection such as east Japan 50Hz system and west Japan 60Hz system, smoothing effect will work very well, and as the result, the author thinks that there will be no scene that batteries work effectively in the matter of fact. But it will be not useless to think how battery should be controlled for LFC.

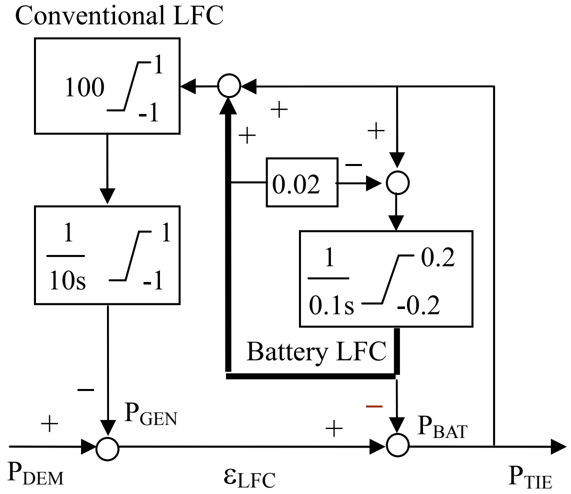

Fig. 1.31 Complementary control of conventional and battery LFC

Since battery LFC is further fast than conventional LFC, its burden tends to concentrate on battery LFC. Battery LFC should compensate residual error of conventional LFC. If it is possible, conventional LFC does not become lazy, and as the result, necessary battery capacity becomes smaller. To realize the hope, a method shown in Fig. 1.31 is effective. Sum of tie line power flow P_{TIE} and battery output P_{BAT} is given to conventional LFC as objective variable. While, only tie line power flow is given to battery LFC as objective variable. As the result, conventional LFC operates as if battery LFC does not exist.

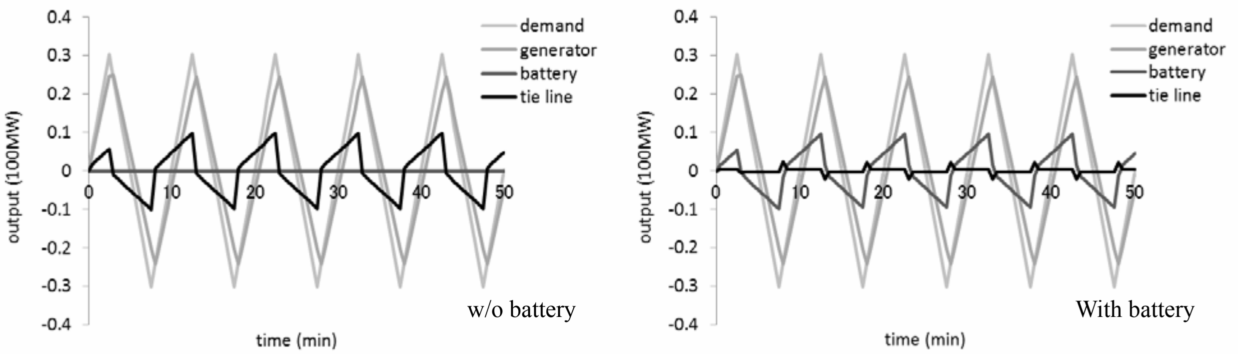

Fig. 1.32 Verification of complementary control of conventional and battery LFC

Simple simulation is done to verify effect of the control. Continuous triangle wave is given as demand fluctuation. Results are shown in Fig. 1.32. Generator output does not change when battery LFC is employed. Tie line power flow without battery turns to battery output when battery is employed. As the result, tie line power flow fluctuation becomes very small when battery is employed. In addition, effects of conventional LFC and battery LFC can be separately recognized.

Is battery LFC useful in existing power system? To answer this question, a simple simulation is performed. Variable output generators are aggregated to a machine. Since ramp rate of existing variable generators' output change is at least 4%/min of their operating output (notice: not rated output) power, ramp rate of the aggregated one machine is also set as 4%/min of operational output power. Assuming that outer system is much larger than the studied system, LFC is simply represented as FTC (Flat Tie line Control). Residual error in LFC becomes larger when idle time along control loop becomes larger. By setting the idle time as 0.5 min, offset has become ±40MW, which appears at normal operation of the studied system.

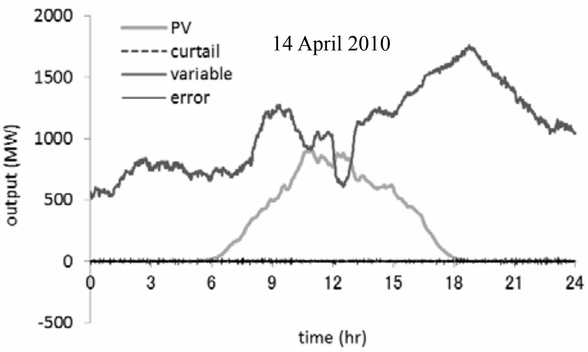

Fig. 1.33 Daily supply with large RE fluctuation

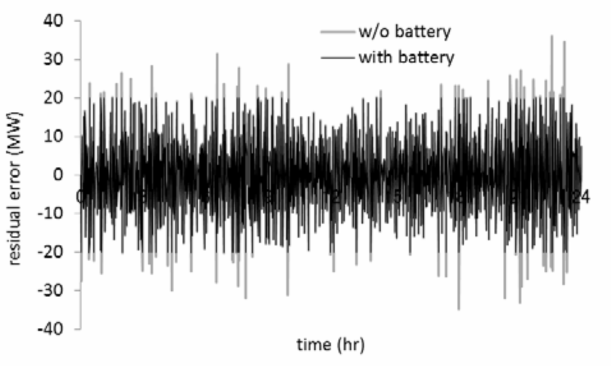

Fig. 1.34 Daily residual error with large RE fluctuation

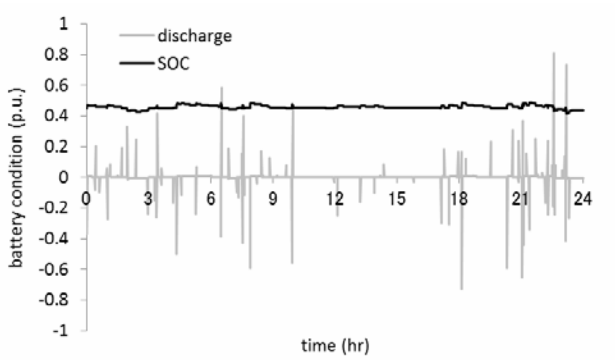

Fig. 1.35 Battery condition with large RE fluctuation

At first in a day with large RE fluctuation, how LFC suffers from RE's fast fluctuation and how battery LFC works usefully are shown in Fig. 1.33, 1.34, and 1.35. 1540MW capacity of PV is assumed. Daily demand variation of the day with largest irradiance fluctuation is used. Variable source has some margin toward minimum output 385MW. Therefore, much residual error does not appear. Although certainly by using battery residual offset is reduced to ±20MW, which is equal to dead band of battery LFC control, this may be excessive power quality.

It is rather fine day that battery LFC becomes useful. Although RE fluctuation is not large, RE output itself is large, therefore, fixed power source is partially curtailed due to excessive electric power. Of course variable source operates at slightly larger power of its minimum output, and its ramp rate become smaller.

When sudden demand decrease happens, conventional LFC nay not be able to follow the change.

Assume 1540MW capacity of PV in a5 May 2010 that is a quite fine day. Minimum output of variable source is 210MW, because one thermal unit is stopped due to demand supply balance. Simulation results are shown in Fig. 1.36, 1.37, and 1.38. Although fixed source is curtailed at most 200MW due to shortage of negative reserve, fixed source output decreases to 224MW and so called "bottoming" occurs. Especially at noon demand decrease much suddenly at bottoming condition, as the result, residual error become -60MW. The error is reduced to -40MW by battery LFC. The difference 20MW is equal to battery LFC capacity. Charge/discharge number of battery is several tens, which is not so hard condition for Lithium ion battery. The small number is brought from adequate offset band width. SOC (State of Charge) of battery rises 0.8 at noon, which is also not so hard condition for Lithium ion battery.

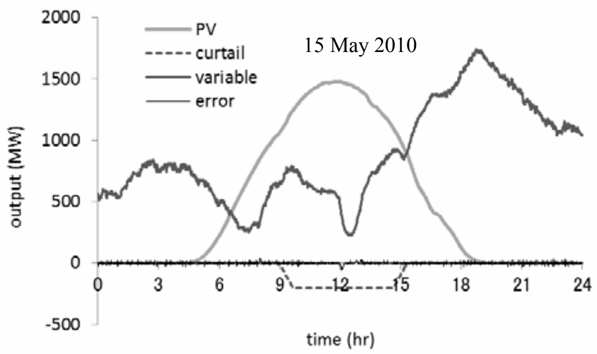

Fig. 1.36 Daily supply on a fine day

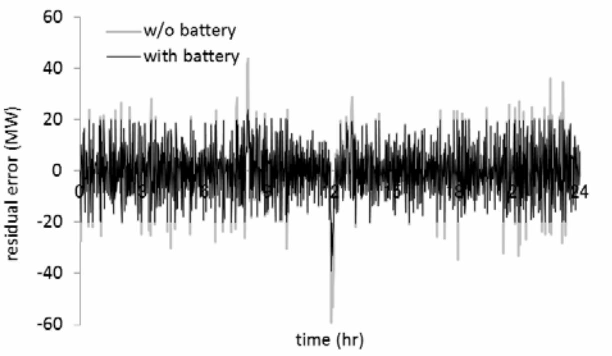

Fig. 1.37 Residual error on a fine day

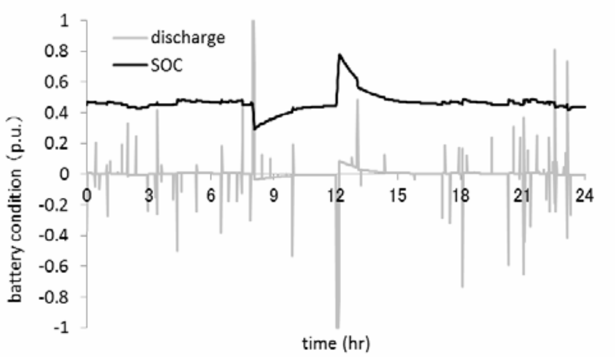

Fig. 1.38 Battery condition on a fine day

As analyzed above, regulation power is prepared at least 4%/min of operating output power of variable source, and t is improbable that fast RE fluctuation impacts tie line power flow harmfully. Therefore, battery will remain as supplementary measure if adopted. Although "Smart Grid" ambition includes usage of new type battery, its necessity must be wisely assessed.

RE Output Prediction

Impact of highly penetrated REs' fluctuation on system frequency regulation seems not so serious as believed in Japan. Impact on system demand supply balance and (positive and negative) reserve rather seems somewhat serious, and some mitigation method will be needed. RE output prediction is regarded as most promising today. The prediction gives RE output several hours to a few days ahead based on weather forecasting data (10 min interval at the shortest), and so on. Since RE output prediction has just stated in

2012 and now proceeding, research result cannot be introduced here. However, rough sketch can be draw as follows.

Roughly saying, next day prediction error of PV is 5 to 10% of rated output as standard deviation σ. The accuracy is the best using such methods as “learning” and so on. System operators consider usually 2σ for 95% reliability. Therefore, prediction error to be considered is 10 to 20%, and become 31MW at most when PVs penetrate 1540MW. The amount is almost rated output of a middle size thermal generator. Although prediction error seems not to be reduced by today’s engineering, it is already known that PV shows much fluctuation in only fine-cloudy day. We can hope that some good method may be found.

By the way, here the author used the words “prediction error”. To calculate prediction error, true value is necessarily needed. Perhaps “RE output identification” will offer approximate value. However, identification method is not established yet in Japan-wide consensus. Since the shortest interval of weather forecast data is 10 min or so, output prediction data ale also given in 10 min interval or so. However, RE output identification already done is based on only such index as “daily maximum 20min fluctuation width” and rich information such as “daily output curve” is not given yet excluding “transfer hypothesis method”, which is not widely accepted in Japan yet. As another identification method, using initial value of prediction can be thought. But, since the method is based on weather data, it must be corrected by something derived from measured irradiance itself.

Ramp Variation of Wind Power Output

It is believed that impact by wind power (WP) is slightly different from PV, that is, slow and large scale ramp variation by such as passing of cold front is more serious than fast cyclic variation. Before analysis of WP ramp variation, WP cyclic variation is once examined.

[WP Cyclic Variation] As an example three WP sites are introduced, which are named as A, B, and C from southwest to northeast. They stand almost on a line with around 70km span. Nominal outputs are 1.8MW, 1.5MW, and 3.0MW respectively. 1/10 decade spectra during January 2007 are shown in Fig. 1.39. Each spectrum is almost flat in faster swing bus slightly decreases by swing speed.

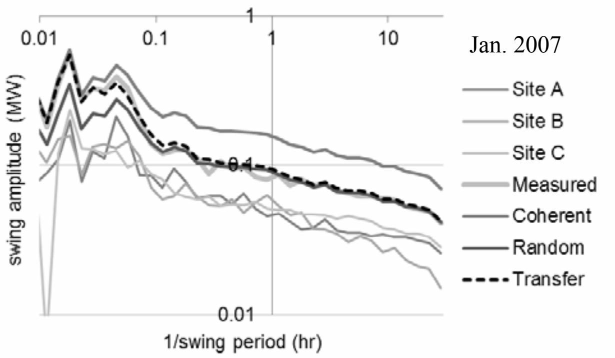

Fig. 1.39 Spectra of the three WP sites

Using swing amplitude at speed f of the three sites: $\varDelta P_A$ (f), $\varDelta P_B$ (f), $\varDelta P_C$ (f), swing amplitude by coherent hypothesis: $\varDelta P_{coh}$ (f) and that of random hypothesis: $\varDelta P_{ran}$ (f) can be calculated as follows.

$$\varDelta P_{coh}(f) = \varDelta P_A(f) + \varDelta P_B(f) + \varDelta P_C(f)$$
$$\varDelta P_{ran}^2(f) = \varDelta P_A^2(f) + \varDelta P_B^2(f) + \varDelta P_C^2(f)$$

Since nominal outputs are different by sites, mutual smoothing effect becomes slightly smaller than the case that all sites have the same rated output. Therefore, instead of site number: N = 3, "equivalent site number: N_{eq} that can be calculated as follows must be used. Here, W_A, W_B, W_C are rated output of these WP sites. As the result, N_{eq} is 2.74 in the case.

$$\frac{1}{\sqrt{N_{eq}}} = \frac{\sqrt{(W_A^2 + W_B^2 + W_C^2)}}{W_A + W_B + W_C} = 0.604218 = \frac{1}{\sqrt{2.73913}}$$

Using the N_{eq}, transfer hypothesis can be expressed as follows.

$$\Delta P_{tra}(f) = \Delta P_{coh}(f) \left| \frac{1 + j\, T_x f / \sqrt{N_{eq}}}{1 + j\, T_x f} \right|$$

Here, T_x is transfer swing period, which is identified so that accumulated square logarithm error between measured value: $\Delta P_{mea}(f)$ and transfer hypothesis: $\Delta P_{tra}(f)$. In this case, T_x = 29.7 hr, which is quite longer than swing period of PV cyclic variation (around 8 hr).

By applying transfer hypothesis, spectrum when much WP with total rated output 1000MW penetrates in Hokuriku region evenly can be presumed as follows. Difference in rated output of the three sites is assumed followed in high penetration.

$$\Delta P_{high}(f) = \Delta P_{mea}(f) \frac{1000\text{MW}}{6.3\text{MW}} \left| \frac{1 + j\, Tx\, f / \sqrt{M_{eq}}}{1 + j\, Tx\, f / \sqrt{N_{eq}}} \right|$$

Here, M_{eq} is equivalent site number of 1000MW penetration case, and is calculated as follows.

$$M_{eq} = N_{eq}\,(6.3\text{MW} / 1000\text{MW})$$

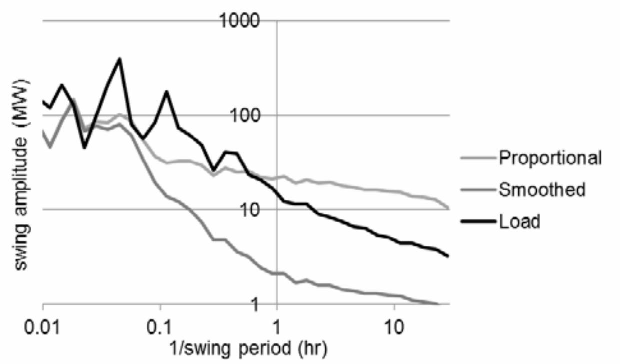

Fig. 1.40　Spectrum of 1000MW WP penetration

Spectrum in 1000MW penetration case considering increased mutual smoothing effect by increased cite number (Smoothed) is shown in Fig. 1.40, in which spectrum without considering the increased mutual smoothing effect (Proportional) and load's cyclic variation spectrum are also shown. Around LFC swing period (1 hr or shorter), "Smoothed" is much smaller than "Load". However, the case assumes that WPs penetrate in even distribution. Considering the fact that suitable region for WP is rather narrower than Hokuriku region, mutual smoothing effect is weaker, and the reality lies between "Smoothed" and

"Proportional". In such a pessimistic assessment, WP cyclic variation shall hardly exceed load variation. As the result, the author agrees with the general opinion that ramp variation is fatal in WP.

[Definition of Ramp Variation] Standard definition is not established yet. Here, definition as Fig. 1.41 is adopted. Ramp variation is defined as increase/decrease in the two time windows with $T_W/2$ width and T_W span. By moving the windows (for example by 1 min notch), ramp values are stored. By the method, number of data hardly decreases, and will good effect for drawing probability density curve afterward. Applying various definition (Japan, Germany, UK, US, and the author), resulted probability density curves are compared in Fig. 1.42 (1). The same three WP sites' data of cyclic variation analysis from Sep. 2006 to Feb. 2007 are adopted.

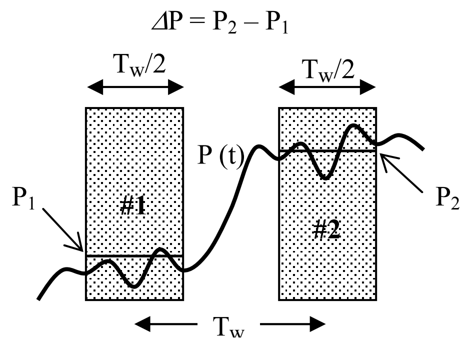

Fig. 1.41 The author's Ramp Definition

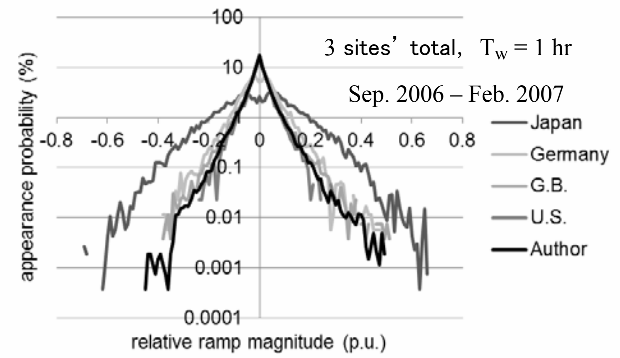

Fig. 1.42 Difference by Ramp Definition

The probability density curve is sometimes called as "umbrella curve" by its form. At a glace, only "Japan" is different, and the other four agree well. Among the four, "Author" curve is continuous even to rarer and larger variation. The character is originated by the fact that data number hardly decreases, and is quite valuable for risk management that needs probability of rare phenomena.

[Difference in Smoothing Effect by Windou Span Tw] Probability curves at window span: T_W =10 hr and Tw = 1 hr are shown in Fig. 1.43. In case of T_W =10 hr, appearance probabilities of each site and the total are almost equal, that is, ramp variation is coherent. On the contrary in case of T_W =10 hr, appearance probability of the total is par less than that of each site, that is, ramp variation is random and mutual smoothing effect is working.

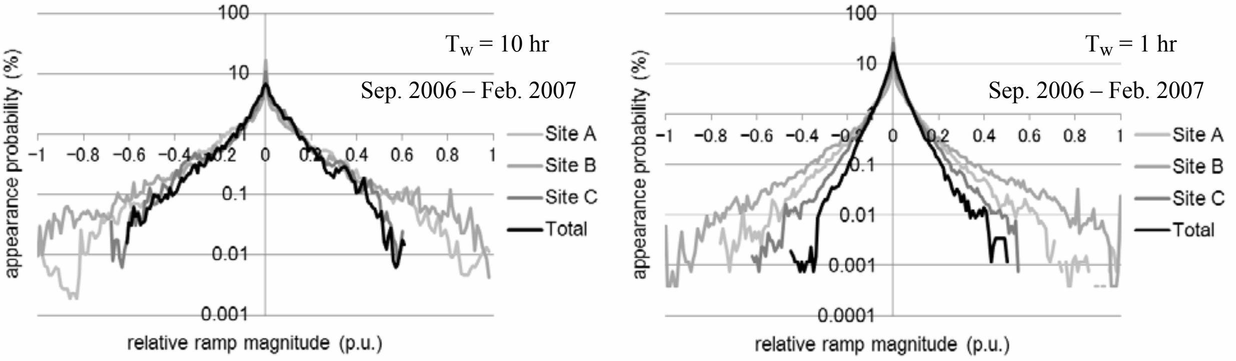

Fig. 1.43 Difference in appearance probability by window span (3 WP sites and the total)

[2σ or 3σ Ramp Magnitude] As a method for quantitative evaluation of mutual smoothing effect in ramp variation, the author proposes "2σ or 3σ ramp magnitude". At first, accumulated probability curves (for both increase and decrease) can be calculated as Fig. 1.44 (example of T_W = 1 hr) from appearance probability curves. Then for various window span T_w, ramp magnitude value over which larger ramp variation never appear with 2σ (95.44%) or 3σ (99.74%) probability can be calculated. Of course, the magnitude value can be calculated for increase or decrease independently. Thus, "2σ or 3σ ramp magnitude" for various T_w can be calculated about each three sites and the total as shown in Fig. 1.45. Also, ramp magnitudes by coherent hypothesis and random hypothesis can be calculated.

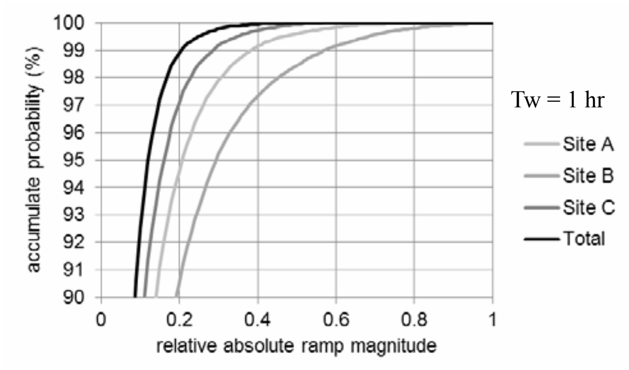

Fig. 1.44 Accumulated probability curves

As the next step, transfer hypothesis is applied. For assessing ramp variation, a constant K is introduced as follows, because a certain weak smoothing effect can be seen even in very slow ramp variation.

$$\Delta P_{tra}(f) = K\,\Delta P_{coh}(f)\left|\frac{1 + j\,T_{wx}\,f / \sqrt{N_{eq}}}{1 + j\,T_{wx}\,f}\right|$$

The identified parameters, which make the accumulated square logarithm error between theoretical value (Transfer) and measured value minimum, are calculated as follows.

2σ ramp magnitude: T_{wx} = 8.74 hr, K = 0.921 3σ ramp magnitude: T_{wx} = 2.74 hr, K = 0.786

Transfer hypothesis agrees with measured value well.

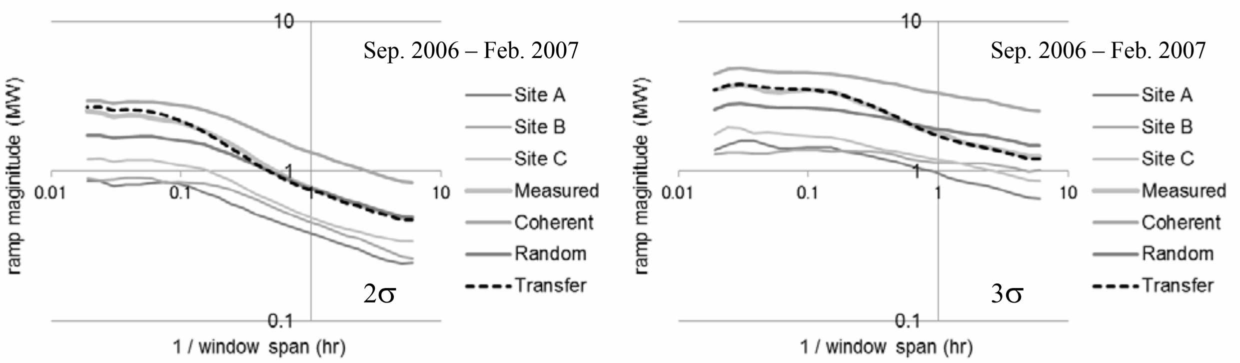

Fig. 1.45 Ramp magnitude by window span (3 WP sites)

Comparing 2σ case and 3σ case, transfer window span T_{wx} is much smaller in 3σ case, that is, mutual smoothing effect works only for shorter window span, and rare slow large ramp variation is hardly smoothed out.

By applying transfer hypothesis, 3σ ramp magnitude by T_w when 1000MW rated output WP penetrates in Hokuriku region by even distribution considering increased mutual smoothing effect (Smoothed) can be presumed as Fig. 1.46. The case without considering the smoothing effect (Proportional) and load's ramp magnitude (Load) are also shown. Calculation method is same as

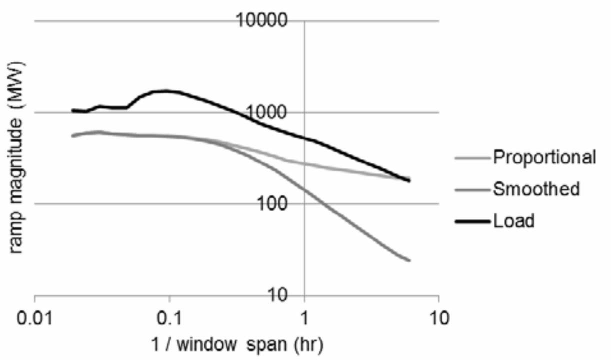

Fig. 1.46 3σ ramp magnitude of 1000MW WP

cyclic variation case. Also load's 3σ ramp magnitude by T_w is shown. It is observed that 1000MW WP's ramp magnitude is far less than load's ramp magnitude. Mutual smoothing effect works well at a few hr T_w or faster.

However, it is too optimistic to feel easy by the fact above. Here, WP sites were assumed to distribute evenly in Hokuriku region. On the contrary in fact, favorable points for WP rather concentrate in a narrower area. As the result, smoothing effect works for only much shorter T_w. Moreover, load can be forecasted with very small error (around 2%) on one hand, on the other hand WP generation can be forecasted with considerably large error (10% by today's arts). Considering those facts above, WP forecast error becomes larger than load forecast error at 1 hr T_w or slower ramp variation. Therefore, it must be pointed out that one of the today's most urgent issues around RE integration is accurate forecast of WP slow but large ramp variation.

Although it has been generally believed that improvement in WP forecast accuracy is fatally important for large WP penetration, it has been not clarified why the improvement is fatally important. By analysis here, it has barely verified that the general belief is correct.

References

(1) Y. Yamagishi, T. Ueda, N. Kanao, & S. Komami: "A Study on the Wind Power Generation Fluctuation of Multiple Sites", IEEJ Trans. PE, Vol. 129, No. 5, pp. 661-667, 2009. (in Japanese)

(2) H. Nagoya, Y. Yamagishi, N. Kanao, & S. Komami: "A Method for Presuming Total Short-term Output Fluctuation of Highly Penetrated Photovoltaic Considering Mutual Smoothing Effect", IEEJ Workshop PE, PE-10-88, 2010. (in Japanese)

(3) H. Nagoya, S. Komami, & K. Ogimoto: "A method for Presuming Total Output Fluctuation of Highly Penetrated Photovoltaic Considering Mutual Smoothing Effect", IEEJ Trans. EIS, Vol. 131, No. 10, pp. 1688-1696, 2011. (in Japanese, to be translated to English in Wiley Online Library)

(4) Y. Yamagishi, H. Nagoya, S. Komami & Y. Fujii: "Estimation of Photovoltaic Generation Output Fluctuation Considering Reduction of Smoothing Effect by Uneven Distribution", IEEJ Trans. EIS, Vol. 131, No. 10, pp.1722-1729, 2011. (in Japanese)

(5) H. Nagoya & S. Komami: "Fundamental Study in a Method for LFC using Battery in Power System with Highly Penetrated Photovoltaic", IEEJ Annual Meeting PE, No. 135, 2011. (in Japanese)

(6) H. Nagoya, S. Komami, & K. Ogimoto: "A Method for Load Frequency Control using Battery in Power System with Highly Penetrated Photovoltaic Generation", IEEJ Trans. PE, Vol. 132, No. 4, pp. 325-333, 2012. (in Japanese)

(7) H. Nagoya, S. Komami, & K. Ogimoto: "A Study in Calculating Output Fluctuation Index of Highly Penetrated Photovoltaic", IEEJ Annual Meeting, No. 6-010, 2012. (in Japanese)

(8) H. Nagoya, S. Komami, and K. Ogimoto: "A Study on Seasonal Trend of Irradiance Fluctuation Profiles on Multiple Sites", National Convention Record IEEJ, No. 6-125, 2013. (in Japanese)

(9) H. Nagoya, S. Komami, K. Ogimoto, and Y. Iwafune: "A Study on Irradiance Fluctuation Profiles of Multiple Sites on Large Fluctuation Days", Annual Conf. of PE, IEEJ, No. 257, 2013. (in Japanese)